Iron Complexes Containing the Ligand *N*,*N*′-Bis(6-methyl-2-pyridylmethyl)-*N*,*N*′-bis(2-pyridylmethyl)ethane-1,2-diamine: Structural, Spectroscopic, and Electrochemical Studies, Reactivity with Hydrogen Peroxide and the Formation of a Low-Spin Fe−OOH Complex

Véronique Balland,[a] Frédéric Banse,*[a] Elodie Anxolabéhère-Mallart,*[a] Martine Nierlich,[b] and Jean-Jacques Girerd*[a]

Keywords: Iron / N ligands / Peroxo ligands / Bioinorganic chemistry

The ligand *N*,*N*′-bis(6-methyl-2-pyridylmethyl)-*N*,*N*′-bis(2-pyridylmethyl)ethane-1,2-diamine ($L_6^2$2M) has allowed to prepare the new Fe^{II} complex [($L_6^2$2M)$FeCl_2$] (**1**), and to compare its structural and spectroscopic characteristics with [($L_6^2$2M)FeCl]PF_6 (**2**). The molecular structure of **1**, resolved by X-ray diffraction, exhibits the ligand tetracoordinated with the two non-methylated pyridine rings coordinated. As shown by UV/Vis spectroscopy and cyclic voltammetry, upon dissolution in methanol or acetonitrile, one chloride ion is released and replaced by a pyridine group. Therefore, complexes **1** and **2** adopt identical structures in solution, i.e. [($L_6^2$2M)$FeCl^+$. However, upon oxidation complex **1** gives several ferric complexes with the ligand $L_6^2$2M pentacoordinated, or tetracoordinated with two chloride ions. This peculiar behaviour is due to the presence of chloride ions in solution in the case of **1**. Upon reaction with H_2O_2 in methanol, complex **2** leads to the formation of low-spin [($L_6^2$2M)$Fe^{III}(OOH)^{2+}$, whereas it is not observed in the case of **1**. Based on the presence or not of chloride ions in solution, a mechanism is proposed for the reactivity of complexes **1** and **2** toward H_2O_2.

Introduction

Dioxygen activation by biological iron-containing systems performing monooxygenation reactions is an attractive sequence since it has considerable scientific and commercial interests. Whatever the system considered, the intermediate responsible for the target reaction, i.e. oxidation of the substrate, is proposed to be a high-valent iron-oxygen species. For mononuclear as well as for dinuclear systems, the events can be schematically described by the same universal sequence: dioxygen reacts with the metal centre(s) in the ferrous state leading to a hydroperoxo ferric complex which then evolves to the high valent entity after O−O bond cleavage. Only in the case of methane monooxygenase (MMO), which contains a non-heme dinuclear active site, has a high valent entity (compound Q), formulated as $Fe^{IV}-(\mu\text{-}O)_2-Fe^{IV}$, been characterised.[1,2] In the case of mononuclear systems with either heme or non-heme active sites, the high valent Fe-oxygen species has not been directly observed, but rather proposed by analogy with compounds I and II of peroxidases which have been identified as Fe^{IV}=O entities.[3]

Evidence has been obtained for the existence of hydroperoxo species, which are the precursors of the fleeting high valent entities, in natural systems such as MMO(dinuclear)[4] and bleomycin (mononuclear),[5] and several synthetic models have also been prepared.[6] To date, no evidence for conversion of a hydroperoxo species to a high valent iron-oxo species in synthetic models has been obtained spectroscopically. However, the recent synthesis of a dinuclear $Fe^{IV}-(\mu\text{-}O)_2-Fe^{IV}$ complex from a mononuclear Fe^{III}-alkylperoxo species[7] shows that such a process may be viable.

In this paper we report the structure and characterisation of a new Fe^{II} complex [($L_6^2$2M)$FeCl_2$] containing the ligand *N*,*N*′-bis(6-methyl-2-pyridylmethyl)-*N*,*N*′-bis(2-pyridylmethyl)ethane-1,2-diamine ($L_6^2$2M). This ligand is a bulkier analogue of the ligand TPEN, which has been shown to give access to a low-spin Fe−OOH intermediate.[8] The behaviour of the new complex [($L_6^2$2M)$FeCl_2$] in solution is considered in detail and its reactivity with H_2O_2 is also presented. We have also investigated the reactivity of the complex [($L_6^2$2M)FeCl]PF_6, previously reported by Bernal et al.,[9] with H_2O_2, and report evidence for the formation of a low-spin Fe−OOH complex from this reaction.

[a] Laboratoire de Chimie Inorganique, UMR CNRS 8613, Université Paris-Sud,
91405 Orsay, France
[b] DRECAM/SCM bat 125, CEA Saclay,
91191 Gif-sur-Yvette, France

Supporting information for this article is available on the WWW under http://www.eurjic.org or from the author.

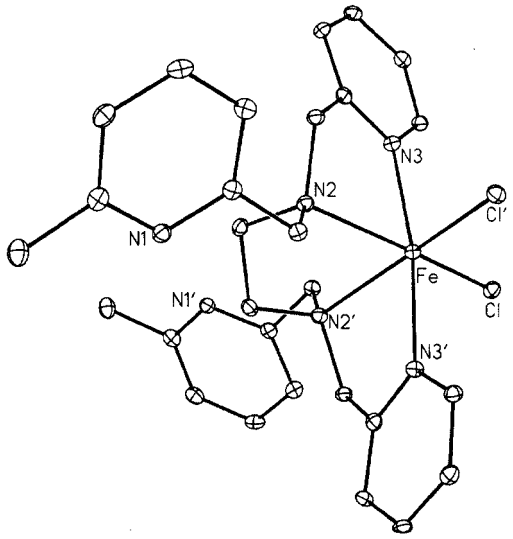

Figure 1. X-ray structure of the molecular complex $[(L_6^2 2M)FeCl_2]$ (**1**)

Results and Discussion

X-ray Crystal Structure

The structure of $[(L_6^2 2M)FeCl_2]$ (**1**) is presented in Figure 1. The Fe^{II} ion has a distorted octahedral geometry with two pyridine nitrogen atoms (N_3) in axial positions and two amino nitrogen atoms (N_2) in equatorial positions. The coordination sphere is completed by two chloride ligands in the equatorial plane.

The potentially hexadentate ligand $L_6^2 2M$ behaves here as a tetradentate ligand with the sterically hindered 6-methylpyridine groups not coordinating to the metal centre. This structure is analogous to those obtained for Fe complexes with tetradentate ligands derived from *N*,*N*′-bis(2-pyridylmethyl)ethane-1,2-diamine.[10−12]

A selection of structural data is reported in Table 1. The Fe−ligand bond lengths are characteristic of a high spin ferrous ion,[12] with the average bond length being 2.256 Å. As expected, the pyridine nitrogen atoms are closer to the Fe than the amino nitrogen atoms (cf. Table 1). The value of ca. 78° for the N_2-Fe-N_2 angle is typical of a five membered metallacycle.[13] Other angles between atoms in the Fe^{II} coordination sphere are also consistent with a strongly distorted octahedral geometry (cf. Table 1).

Table 1. Selected bond lengths and angles for $[(L_6^2 2M)FeCl_2]$ (**1**)

Bond lengths [Å]		Bond angles [°]	
Fe−N_2	2.320 (3)	N_2-Fe-N_2	78.18 (15)
Fe−N_3	2.192 (3)	N_3-Fe-N_3	170.90 (16)
Fe−Cl	2.4276 (10)	Cl−Fe−Cl	106.24 (5)

Table 2. UV/Vis data for $[(L_6^2 2M)FeCl_2]$ (**1**), $[(L_6^2 2M)FeCl]^+$(**2**), and some similar complexes in acetonitrile and methanol; abbreviations used for the ligands: L_5^2 = *N*-methyl-*N*,*N*′,*N*′-tris(2-pyridylmethyl)ethane-1,2-diamine; L_5^+ = *N*,*N*′,*N*′-tris(2-pyridylmethyl)-*N*′-trimethylammoniopentyl-ethane-1,2-diamine; trispicen = *N*,*N*′,*N*′-tris(2-pyridylmethyl)ethane-1,2-diamine; $LBzl_2$ = *N*,*N*′-dibenzyl-*N*,*N*′-bis(2-pyridylmethyl)ethane-1,2-diamine; L_4^2 = *N*,*N*′-dimethyl-*N*,*N*′-bis(2-pyridylmethyl)ethane-1,2-diamine

Complexes	λ_{max} [nm], ε [$M^{-1}cm^{-1}$]	
	CH_3CN	CH_3OH
$[(L_6^2 2M)FeCl_2]$	388, 1700	381, 1700
$[(L_6^2 2M)FeCl]PF_6$	378, 1700	376, 1700
$[(L_5^2)FeCl]PF_6$ [9]	399, 1840	
$[(L_5^+)FeCl](ClO_4)_2$ [14]	398, 1600	
$[(L_5^2)FeCl]Cl$[15]		385, 1750
[(trispicen)FeCl]PF_6 [8]		395, 1900
$[(LBzl_2)FeCl_2]$[12]	411, 1180	
$[(L_4^2)FeCl_2]$[16]	415, 770	

UV/Vis Spectroscopy

The electronic spectra of complexes $[(L_6^2 2M)FeCl_2]$ (**1**) and $[(L_6^2 2M)FeCl]PF_6$ (**2**) have been recorded in both acetonitrile and methanol, and the data are summarised in Table 2. The spectroscopic characteristics of both **1** and **2** are very similar in both solvents. In each case, the spectrum is dominated by an intense band in the UV corresponding to a pyridine π−π* transition (not reported in Table 2) and another at ca. 400 nm that is attributed to a Fe^{II}-to-pyridine MLCT transition. The ε values for the latter are characteristic of high-spin Fe^{II} systems.[14]

The fact that both $[(L_6^2 2M)FeCl_2]$ and $[(L_6^2 2M)FeCl]^+$ display similar spectra in solution suggests that they adopt a similar structure. Moreover, it is very likely that no solvent molecule is involved in the coordination sphere since the spectra obtained are identical in CH_3OH and CH_3CN.

The spectrum of $[(L_6^2 2M)FeCl_2]$ is different to that of $[(LBzl_2)FeCl_2]$ (cf. Table 2) and related complexes with a $[LFeCl_2]$ structure (L designates a tetradentate aminopyridine ligand).[12,16] These usually display a MLCT band at ca. 410 nm in acetonitrile. In contrast, $[(L_6^2 2M)FeCl_2]$ displays a MLCT band whose position and intensity are very similar to those observed for $[(L_6^2 2M)FeCl]PF_6$ (cf. Table 2) and similar complexes with three pyridines and an ethanediamine fragment.[8,9,14,15,17] The data reported for high spin Fe^{II} complexes with ethane-1,2-diamine/pyridine ligands show that the ε value of the MLCT band appears to correlate with the number of coordinated pyridines; for example, $\varepsilon \approx 1000\ M^{-1}cm^{-1}$ for complexes with two pyridines bound to Fe^{II} [12,16] while those with three pyridines bound to Fe^{II} [8,9,14,15,17] have $\varepsilon \approx 1600-2000\ M^{-1}cm^{-1}$.

It is also possible to compare the λ_{max} of the MLCT for *bis*-chloro complexes containing a tetradentate ligand ($\lambda_{max} \approx 410$ nm) with *mono*-chloro complexes containing a pentadentate ligand ($\lambda_{max} \approx 380$ nm). Substituting a π donor Cl^-, which destabilises the t_{2g} set of d orbitals, with a π accepting pyridine, which stabilises the t_{2g} set, will increase the gap between the t_{2g} metal orbitals and the pyri-

dine π* orbitals thus resulting in a shift of the λ_{max} of the MLCT to shorter wavelength.

Both the λ_{max} of ca. 380 nm and the ε value of 1700 $M^{-1}cm^{-1}$ obtained for $[(L_6^2 2M)FeCl_2]$ are thus consistent with a structure where three pyridines are coordinated to the metal. The neutral structure observed in the solid state by X-ray diffraction is therefore not maintained in CH_3CN or CH_3OH solution since a chloride ligand is displaced by one of the pendant pyridines.

Cyclic Voltammetry

The cyclic voltammograms of $[(L_6^2 2M)FeCl]PF_6$ and $[(L_6^2 2M)FeCl_2]$ recorded at 20 °C in acetonitrile are presented in Figure 2.

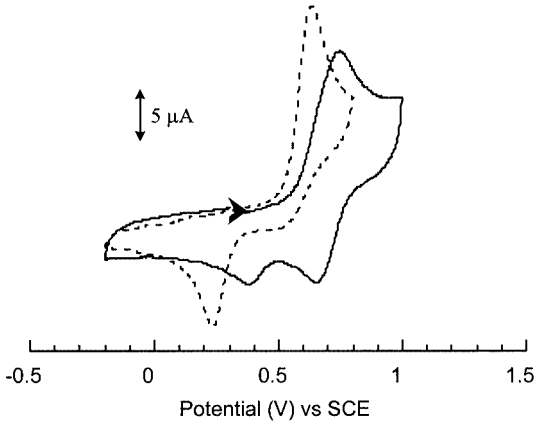

Figure 2. Cyclic voltammograms of $[(L_6^2 2M)Fe^{II}Cl]PF_6$ (**2**) (−) and $[(L_6^2 2M)Fe^{II}Cl_2]$ (**1**) (- - -) in acetonitrile at 20 °C

The cyclic voltammogram of $[(L_6^2 2M)FeCl]PF_6$ is analogous to the one previously reported by Bernal et al. for the same complex.[9] It exhibits one broad quasi-reversible wave with $E_{1/2}$ = 0.70 V (ΔE_p = 100 mV) and an extra cathodic wave at 0.38 V on the reverse scan. The broad quasi-reversible response corresponds to oxidation of $[(L_6^2 2M)Fe^{II}Cl]^+ \rightarrow [(L_6^2 2M)Fe^{III}Cl]^{2+}$. The second cathodic peak can be attributed to the reduction of a species obtained after rapid transformation of $[(L_6^2 2M)Fe^{III}Cl]^{2+}$ generated at the electrode. Indeed, the intensity of this last wave is decreased when the scan rate is increased. By analogy with the electrochemical behaviour of $[(L_5^3)Fe^{II}Cl]^+$ (L_5^3 = *N*-Methyl-*N*,*N*′,*N*′-tris(2-pyridylmethyl)propane-1,3-diamine) in CH_3OH[13] we propose that this transient complex can be formulated as $[(L_6^2 2M)Fe^{III}(OH)]^{2+}$, with the OH^- coming from residual water in the supporting electrolyte (see Exp. Sect.).

As depicted in Figure 2, $[(L_6^2 2M)FeCl_2]$ displays completely irreversible electrochemistry, with the anodic wave at E_{ox} = 0.63 V and a cathodic wave at 0.23 V. The oxidation potential of 0.63 V is close to that of $[(L_6^2 2M)Fe^{II}Cl]PF_6$ (E_{ox} = 0.75V; cf. Figure 2). This observation is in agreement with the conclusions drawn from the UV/Vis spectra (see above), i.e. formation of $[(L_6^2 2M)Fe^{II}Cl]^+$ from $[(L_6^2 2M)Fe^{II}Cl_2]$ in solution. Moreover, the one electron $Fe^{II} \rightarrow Fe^{III}$ oxidation observed for neutral $[LFeCl_2]$ complexes {L = *N*,*N*′-di-R-*N*,*N*′-bis(2-pyridylmethyl)ethane-1,2-diamine (R = H, Me, benzyl)} is usually reversible in acetonitrile, with $E_{1/2}$ values in the range 0.045−0.232 V vs. SCE,[10,12,18,19] significantly lower than the value of 0.63 V observed here. For example, the neutral complex $[L_4^2 Fe^{II}Cl_2]$ {L_4^2 = *N*,*N*′-dimethyl-*N*,*N*′-bis(2-pyridylmethyl)-ethane-1,2-diamine} has $E_{1/2}$ = 0.18 V.[19] The value of 0.63 V indicates that neutral $[(L_6^2 2M)Fe^{II}Cl_2]$ rearranges to $[(L_6^2 2M)Fe^{II}Cl]Cl$ in acetonitrile, in agreement with UV/Vis spectroscopy studies. In contrast, the wave at 0.23 V on the reverse scan is characteristic of the reduction of the bis chloro complex $[(L_6^2 2M)Fe^{III}Cl_2]^+$.

The lower E_{ox} potential value for complex **1** (0.63 V) compared to complex **2** (0.75 V) suggests the existence of a rapid chemical reaction subsequent to the electron transfer (EC mechanism).[20] Variation of the scan rate between 50 and 500 mV/s had no influence on the shape of the voltammogram, indicating that even the fastest scan rate was in-

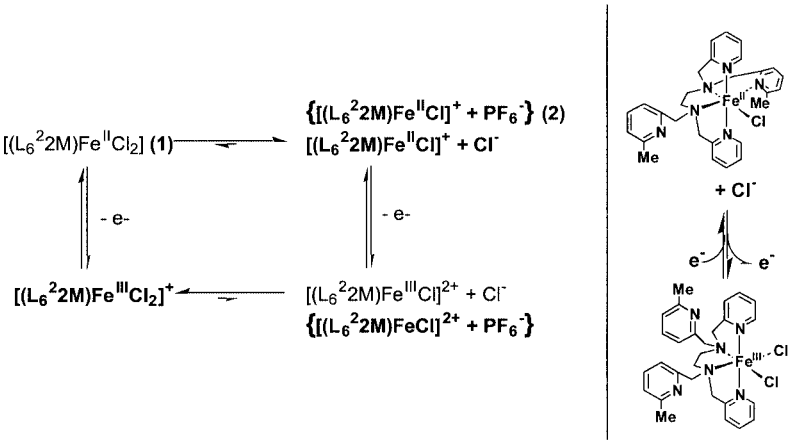

Scheme 1. Summary of electrochemical results for $[(L_6^2 2M)FeCl_2]$ (**1**) and $[(L_6^2 2M)FeCl]PF_6$ (**2**) in acetonitrile; species detected appear in bold characters; the second ferric complex detected in the cyclic voltammogram of **2** (see text) has been neglected here; the right part illustrates the EC mechanism observed for **1**

sufficiently rapid to allow observation of the fast chemical reaction following the electron transfer. From the above observations, we propose that this chemical reaction is the rapid complexation of the Fe^{III} species by free Cl^- ions, thus generating the $[(L_6^22M)Fe^{III}Cl_2]^+$ complex, in which the ligand is tetradentate with two pendant pyridines. Indeed the oxidation wave of free Cl^- is not observed even at 500 mV/s.

The results obtained from the electrochemical studies are summarised in Scheme 1. Dissolution of $[(L_6^22M)Fe^{II}Cl_2]$ (**1**) in acetonitrile immediately gives $[(L_6^22M)Fe^{II}Cl]^+$. When oxidised, this complex gives the unstable ferric analog which then interacts immediately with the free Cl^- to give $[(L_6^22M)Fe^{III}Cl_2]^+$ in which the ligand L_6^22M is tetradentate. This latter complex is reduced at 0.23V.

In the case of $[(L_6^22M)FeCl]PF_6$ (**2**), no extra Cl^- is available in solution to react with $[(L_6^22M)FeCl]^{2+}$ in which the L_6^22M ligand coordinates in a pentadentate fashion. As a matter of fact, this latter ferric complex is stable and can be easily detected. These electrochemical studies suggest that, although both complexes adopt the same structure at the ferrous level, they give different species on oxidation.

The electrochemical behaviour of these two complexes was also investigated in CH_3OH, and in both cases, the Fe^{II}/Fe^{III} system is completely irreversible. The complex $[(L_6^22M)Fe^{II}Cl]PF_6$ (**2**) reacts rapidly to form $[(L_6^22M)Fe^{III}(OCH_3)]^{2+}$ and $[(L_6^22M)Fe^{III}(OH)]^{2+}$. Such behaviour has already been observed for complexes with similar pentadentate ligands.[13,21] This indicates that the chloride ion is easily substituted in CH_3OH when the complex is in its ferric state. Following oxidation of $[(L_6^22M)Fe^{II}Cl_2]$ (**1**), the complexes $[(L_6^22M)Fe^{III}(OCH_3)]^{2+}$ and $[(L_6^22M)Fe^{III}(OH)]^{2+}$ are observed as for **2**. However, a third cathodic wave is detected at a lower potential (ca. 12 mV, see Supporting Information). By analogy with the study in CH_3CN, this latter wave is attributed to the reduction of $[(L_6^22M)Fe^{III}Cl_2]^+$. The chloride ions have such a high affinity for Fe^{III} even in CH_3OH that for $Cl^-/Fe = 2$, the bis-chloro-Fe^{III} complex is obtained.

Reactivity with H_2O_2

The reactivities of the complexes $[(L_6^22M)FeCl_2]$ and $[(L_6^22M)FeCl]PF_6$ with an excess of H_2O_2 was studied in CH_3OH by using a variety of techniques.

The reaction of H_2O_2 with $[(L_6^22M)FeCl]PF_6$ has previously been studied by Bernal et al. but no intermediate was clearly identified.[9] We present here a reinvestigation of this reaction. Addition of 100 equivalents of H_2O_2 to $[(L_6^22M)FeCl]PF_6$ in methanol at −40 °C resulted in the appearance of a low intensity band at 530 nm in the UV/Vis spectrum. This is attributed to a hydroperoxo-to-Fe^{III} charge transfer transition, with an energy similar to other low-spin $Fe^{III}-OOH$ species involving a ligand containing three pyridines coordinated to the metal.[6] The low intensity of the band indicates either a low conversion to Fe−OOH or a high instability of the hydroperoxo product. The maximum intensity is observed after ca. one hour (at −40 °C), which reflects a steady state for this intermediate, due to the large excess of H_2O_2. Similar behaviour was observed for $[(TPEN)FeCl]^+$ {TPEN = *N*,*N*,*N*′,*N*′-tetrakis(2-pyridylmethyl)ethane-1,2-diamine}, but a much more stable $Fe^{III}-OOH$ intermediate was obtained at room temperature.[8]

The EPR spectrum of the solution was recorded at 4 K. It exhibits several resonances that arise from more than one species (cf. Figure 3). A $g = 4.2$ signal is attributed to a high spin Fe^{III} degradation species (not shown in Figure 3).[22] Other resonances around $g = 2$ are characteristic of low-spin Fe^{III} complexes. Two sets of very close g values can be distinguished with $g_{max} = 2.2$ or 2.18; $g_{inter} = 2.12$ and 2.12; $g_{min} = 1.97$ or 1.96. Starting with the complex $[(L_6^22M)Fe(OH_2)](PF_6)_2$, Bernal et al. have observed identical values.[9] These sets of g values are characteristic of low-spin Fe^{III} in nearly axial symmetry, and are consistent with EPR data reported for low-spin $Fe^{III}-OOH$ entities.[6] For example, the Fe^{III} complex of the TPEN ligand exhibits g values of 2.22, 2.15, and 2.00.[8]

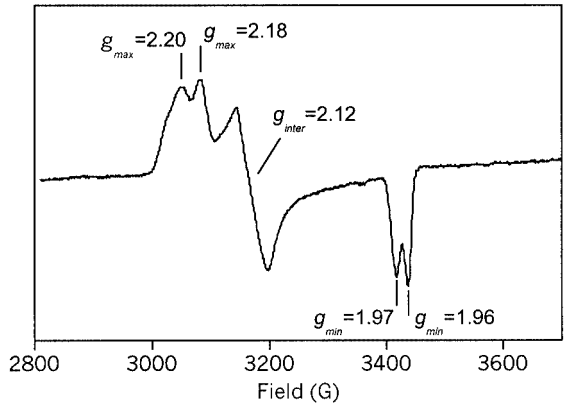

Figure 3. EPR spectrum of a mixture of $[(L_6^22M)Fe^{II}Cl]PF_6$ (**2**) and 100 equivalents of H_2O_2 in CH_3OH at 4 K

The simplest way to rationalise the presence of two close but different sets of g values is to propose two different coordination modes for the ligand L_6^22M. Indeed, the ratio of coordinated pyridines to coordinated methylated pyridines can be 1:2 or 2:1 when this ligand coordinates in a pentadentate fashion, as represented in Scheme 2.

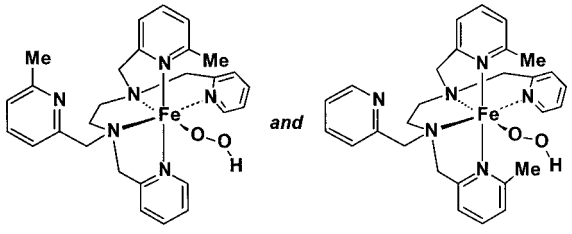

Scheme 2. Proposed structures for the two low-spin intermediates of formula $[(L_6^22M)Fe(OOH)]^{2+}$

Starting with the complex $[(L_6^22M)FeCl_2]$ (**1**), no reaction intermediate was observed by UV/Vis spectroscopy at −40 °C even though it adopts a structure in solution ident-

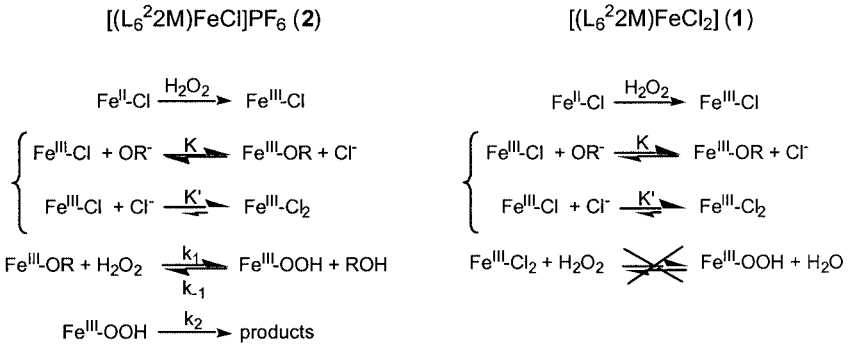

Scheme 3. Mechanism proposed for the reactivity toward H_2O_2 of complexes **1** and **2** (R=H or CH_3)

ical to that of complex **2** i.e. $[(L_6^22M)Fe^{II}Cl]^+$ (see above). The only difference between **1** and **2** is the presence of chloride ions in solution in the case of **1**. As shown by electrochemistry, oxidation of complex **1** leads to the formation of $[(L_6^22M)Fe^{III}Cl_2]^+$, in which the ligand coordinates in a tetradentate fashion. To the best of our knowledge, no reaction intermediate has ever been reported upon addition of H_2O_2 to a complex containing a linear tetracoordinate ligand.

The fact that $[(L_6^22M)FeCl]PF_6$ (**2**) but not $[(L_6^22M)FeCl_2]$ (**1**) has allowed to observe a low-spin mononuclear Fe−OOH intermediate, substantiates the mechanism we proposed for the formation of Fe−OOH intermediates.[13] In this paper, adjustment of kinetic data was made by considering very fast pre-equilibria to give a mononuclear Fe^{III} complex upon oxidation of the Fe^{II} precursor.[13] Here we propose that $[(L_6^22M)FeCl_2]$ is not able to give a mononuclear Fe−OOH complex since the ferric complex obtained contains the ligand L_6^22M bound in a tetradentate fashion following substitution of a pyridyl arm by a free chloride ion (cf. Scheme 3).

The statement that a mononuclear Fe−OOH is not obtained from complex **1** may not be rigorously true. Indeed, when complex **1** is oxidised in CH_3OH, it also gives the Fe^{III}−OH and Fe^{III}−OCH_3 complexes as in the case of **2**. These species are precursors of the Fe−OOH complex (cf. Scheme 3). However, since the conversion of **2** into the Fe−OOH is low as noted above, it will be even lower starting from complex **1**, and not observable under these experimental conditions.

Conclusion

We have synthesised two Fe^{II} complexes of the ligand L_6^22M. The crystal structure of neutral $[(L_6^22M)FeCl_2]$ (**1**) shows two chloride ions coordinated to the metal centre in *cis* positions and the potential hexadentate ligand coordinated in a tetradentate fashion. The complex $[(L_6^22M)FeCl]PF_6$ (**2**) contains the ligand bound in a pentacoordinate fashion, as revealed by UV/Vis and cyclic voltammetry. However, it probably exhibits two different coordination modes, with one pendant pyridine which may be either methylated or not methylated. Upon dissolution in acetonitrile or methanol, one chloride ion of $[(L_6^22M)FeCl_2]$ (**1**) is replaced by a nitrogen atom of a methylated pyridine group. Therefore, the two Fe^{II} complexes adopt similar structures in solution. Upon electrochemical oxidation in acetonitrile, $[(L_6^22M)FeCl]PF_6$ (**2**) gives its ferric analog whereas $[(L_6^22M)FeCl_2]$ (**1**) is subject to a fast EC mechanism to give $[(L_6^22M)Fe^{III}Cl_2]^+$ in which the ligand is tetracoordinate. When oxidised in MeOH, both **1** and **2** give $[(L_6^22M)Fe^{III}(OR)]^{2+}$ (R = H or CH_3), but a third complex, $[(L_6^22M)Fe^{III}Cl_2]^+$, is also observed for **1** with the ligand bound tetradentate.

These different structures at the Fe^{III} oxidation state are probably responsible for the different reactivities in the presence of H_2O_2. Two similar low-spin Fe^{III}−OOH intermediates have been characterised for $[(L_6^22M)FeCl]PF_6$ (**2**) upon reaction with H_2O_2 at −40 °C. These two Fe^{III}−OOH species very likely differ only in the number of coordinated methylated pyridines. The complexes reported here are unstable when compared to Fe^{III}−OOH complexes obtained with similar ligands. Compared to the parent ligand TPEN[8] the instability observed here may be related to the bulkiness of the L_6^22M ligand. Indeed it is likely that this ligand is not well adapted to the small Fe^{III} ion, due to steric congestion provided by the pyridine rings.

Starting from $[(L_6^22M)FeCl_2]$ (**1**) in MeOH, no intermediate could be detected under the same experimental conditions.

Although both Fe^{II} complexes have analogous structures in solution, their reactivities in the presence of H_2O_2 are different. This clearly establishes that the $Fe^{II} \rightarrow Fe^{III}$ oxidation is the first process occurring during the reaction between a ferrous complex and H_2O_2. The HOO^- ligand then reacts with the ferric complex obtained. The observations reported in this paper confirm the mechanism proposed to analyse the kinetic data of a similar low-spin Fe^{III}−OOH complex.[13]

Experimental Section

Materials: Starting materials were purchased from Acros. Solvents were purchased from Merck and used without further purification.

Synthesis of *N,N′*-bis(6-methyl-2-pyridylmethyl)-*N,N′*-bis(2-pyridylmethyl)ethane-1,2-diamine ($L_6^2$2M): This ligand was prepared following the method reported by Toftlund and Yde-Andersen.[23]

Synthesis of [($L_6^2$2M)$FeCl_2$] (1): This synthesis was performed by using Schlenk tubes and a vacuum-argon line. A solution of $L_6^2$2M (140 mg) in THF was added to a solution of $FeCl_2{\cdot}2H_2O$ (50 mg, 1.01 equiv.) in THF (10 mL) and a yellow powder rapidly precipitated. The reaction mixture was stirred for 30 minutes, the solvent was partially removed and the powder was isolated by filtration. Yield 86 mg (48%). Crystals suitable for structural determination were obtained by slow diffusion of *tert*-butyl methyl ether into an acetonitrile solution of the complex. Elemental analysis, found: C 58.43, H 5.30, Cl 12.47, N 14.15; calculated for $C_{28}H_{32}Cl_2FeN_6$ (579.4): C 58.12, H 5.58, Cl 12.1, N 14.53.

Synthesis of [($L_6^2$2M)FeCl]PF_6 (2): This synthesis was performed under an argon atmosphere as for complex **1** following the method reported by Bernal et al.[9] A methanol solution of $L_6^2$2M (515 mg) was added to a solution of $FeCl_2{\cdot}2H_2O$ (185 mg, 1 equiv.) in methanol (5 mL). The yellow solution was stirred for 15 minutes and $NaPF_6$ (200 mg, 2 equiv.) in methanol was then added. The majority of the solvent was removed and of to give a yellow powder. Yield 470 mg (50%). Elemental analysis, found: C 38.44, H 4.07, N 9.67; calculated for $C_{28}H_{32}N_6FeClPF_6{\cdot}NaPF_6{\cdot}H_2O$ (874.8): C 38.44, H 3.92, N 9.61.

Physical Measurements: Elemental analyses were performed by the Service Central d'Analyses du CNRS (Vernaison-France). UV/Vis spectra were recorded on a Varian Cary 300 Bio spectrophotometer at 20 °C with 1 cm quartz cuvettes. Stopped-flow experiments were performed with a Biologic SFM-300 equipped with a Julabo F 30C cryostat. Spectra were recorded in the range 200−1022 nm with a 0.5 cm optical path and a 50 μL cuvette. The delay after mixing is 3 ms. Cyclic Voltammograms were measured using an EGG PAR model M270 scanning potentiostat operating at scan rates of 10−1000 $mV{\cdot}s^{-1}$. Studies were carried out under an argon atmosphere in acetonitrile or methanol solutions using 0.2 M tBu_4NClO_4 (puriss grade, Fluka) as the supporting electrolyte, and 10^{-3} M of the complex. In order to minimise the amount of water contained in the system, the supporting electrolyte solution was dried over Al_2O_3 prior to use. The working electrode was a glassy carbon disk (0.32 cm^2) polished with 1 μm diamond paste. The reference electrode was Ag-$AgClO_4$ (0.3 V vs. SCE electrode) separated from the test solution by a salt bridge containing the solvent/supporting electrolyte, with a gold auxiliary electrode. All potentials are given vs. SCE electrode (0.241 V vs. NHE electrode).

Crystallographic Data Collection: The data were collected on a Nonius−Kappa-CCD area detector diffractometer by using graphite-monochromated Mo-K_α radiation. The lattice parameters were determined from ten images recorded with 2° -scans and later refined on all data. The data were recorded at 123 K. A 180° -range was scanned with 2° steps with a crystal to detector distance fixed at 30 mm. Data were corrected for Lorentz polarisation. The structure was solved by direct methods by using SHELXS[24] and refined by full-matrix least-squares on F^2 with anisotropic thermal parameters for all non H atoms using SHELXL-97.[25] H atoms were introduced at calculated positions as riding atoms with an isotropic displacement parameter equal to 1.2 (CH and CH_2) times that of the parent atom. The molecular plots were drawn by using SHELXTL.[26] All calculations were performed on a Silicon Graphics R10000 workstation. The crystal data and parameters for data collection are summarised in Table 3.

CCDC-199948 contains the supplementary crystallographic data for this paper. These data can be obtained free of charge at www.ccdc.cam.ac.uk/conts/retrieving.html [or from the Cambridge Crystallographic Data Centre, 12, Union Road, Cambridge CB2 1EZ, UK; Fax: (internat.) +44−1223/336-033; E-mail: deposit@ccdc.cam.ac.uk].

Supporting Information (see footnote on the first page of this article): Voltammograms of complexes (**1**) (- - -) and (**2**) (−) in CH_3OH at 20 °C.

Table 3. Summary of X-ray crystallographic data for [($L_6^2$2M)$FeCl_2$] (**1**)

Empirical formula	$C_{28}H_{32}Cl_2FeN_6$
Formula mass	579.35
Crystal system	orthorhombic
space group	Pbcn
a [Å]	12.548(3)
b [Å]	10.046(2)
c [Å]	21.009(4)
V [Å^3]	2648.3(9)
Z	4
D(calcd.) [g/cm^3]	1.453
μ [cm^{-1}]	0.801
Crystal size [mm]	0.15 × 0.10 × 0.10
Radiation type	Mo-*K*α
Temperature [K]	123(2)
θ range [deg]	2.53−24.67
No. of reflns. collected	16004
No. of reflns. merged	2107
No. of reflns. obsd.	1648
Observation criterion	$I > 2\sigma(I)$
no of params refined	168
R[a]	0.0458
R_w[b]	0.0968
Goodness of fit	0.932

[a] $R = \Sigma(||F_o| - |F_c||)/\Sigma|F_o|$. [b] $R_w = [\Sigma w(||F_o| - |F_c||)^2/\Sigma w(|F_o|)^2]^{1/2}$.

[1] M. Merkx, D. A. Kopp, M. H. Sazinsky, J. L. Blazyk, J. Müller, S. J. Lippard, *Angew. Chem. Int. Ed.* **2001**, *40*, 2782.
[2] B. J. Wallar, J. D. Lipscomb, *Chem. Rev.* **1996**, *96*, 2625.
[3] B. Meunier, J. Bernadou, in: *Structure and Bonding, Vol. 97* (Ed.: B. Meunier), **2000**, pp. 1.
[4] J. DuBois, T. J. Mizoguchi, S. J. Lippard, *Coord. Chem. Rev.* **2000**, *200−202*, 443.
[5] R. M. Burger, in: *Structure and Bonding, Vol. 97* (Ed.: B. Meunier), **2000**, pp. 287.
[6] J. J. Girerd, F. Banse, A. J. Simaan, in: *Structure and Bonding, Vol. 97* (Ed.: B. Meunier), **2000**, pp. 146.
[7] M. Costas, J.-U. Rohde, A. Stubna, R. Y. N. Ho, L. Quaroni, E. Münck, L. Que, *J. Am. Chem. Soc.* **2001**, *123*, 12931.
[8] A. J. Simaan, S. Döpner, F. Banse, S. Bourcier, G. Bouchoux, A. Boussac, P. Hildebrandt, J. J. Girerd, **2000**, *Eur. J. Inorg. Chem.* 1627.
[9] I. Bernal, I. M. Jensen, K. B. Jensen, C. J. McKenzie, H. Toftlund, J. P. Tuchagues, *J. Chem. Soc., Dalton Trans.* **1995**, 3667.
[10] N. Arulsamy, D. J. Hodgson, J. Glerup, *Inorg. Chim. Acta* **1993**, *209*, 61.
[11] K. Chen, L. Que, *Chem. Commun.* **1999**, 1375.
[12] A. J. Simaan, S. Poussereau, G. Blondin, J. J. Girerd, D. Defaye, C. Philouze, J. Guilhem, L. Tchertanov, *Inorg. Chim. Acta* **2000**, *299*, 221.
[13] V. Balland, F. Banse, E. Anxolabéhère-Mallart, M. Ghiladi, T. Mattioli, C. Philouze, G. Blondin, J.-J. Girerd, *Inorg. Chem.*, in press.

[14] P. Mialane, A. Novorojkine, G. Pratviel, L. Azéma, M. Slany, F. Godde, A. Simaan, F. Banse, T. Kargar-Grisel, G. Bouchoux, J. Sainton, O. Horner, J. Guilhem, L. Tchertanova, B. Meunier, J. J. Girerd, *Inorg. Chem.* **1999**, *38*, 1085.
[15] A. J. Simaan, F. Banse, P. Mialane, A. Boussac, S. Un, T. Kargar-Grisel, G. Bouchoux, J. J. Girerd, *Eur. J. Inorg. Chem.* **1999**, 993.
[16] N. Raffard, PhD thesis, Université Paris XI (Orsay), **2002**.
[17] A. Hazell, C. J. McKenzie, L. P. Nielsen, S. Schindler, M. Weitzer, *J. Chem. Soc., Dalton Trans.* **2002**, 310.
[18] A. Nivorozhkin, E. Anxolabéhère-Mallart, P. Mialane, R. Davydov, J. Guilhem, M. Cesario, J.-P. Audière, J.-J. Girerd, S. Styring, L. Schussler, J.-L. Seris, *Inorg. Chem.* **1997**, *36*, 846.
[19] N. Raffard, V. Balland, J. Simaan, S. Létard, M. Nierlich, K. Miki, F. Banse, E. Anxolabéhère-Mallart, J.-J. Girerd, *C. R. Chimie* **2002**, *5*, 99.
[20] A. J. Bard, L. R. Faulkner, *Electrochimie; principes, méthodes et applications*, Masson, Paris - New York - Barcelona - Milano - Mexico - Sao Paulo, **1983**.
[21] L. Duelund, R. Hazell, C. J. McKenzie, L. P. Nielsen, H. Toftlund, *J. Chem. Soc., Dalton Trans.* **2001**, 152.
[22] A. J. Simaan, F. Banse, J. J. Girerd, K. Wieghardt, E. Bill, *Inorg. Chem.* **2001**, *40*, 6538.
[23] H. Toftlund, S. Yde-Andersen, *Acta Chem. Scand., Ser. A* **1981**, *35*, 575.
[24] G. M. Sheldrick, *Acta Crystallogr., Sect. A* **1990**, *46*, 467.
[25] G. M. Sheldrick, *SHELXL-97: Program for the Refinement of Crystal Structures*, University of Göttingen, Germany, **1997**.
[26] G. M. Sheldrick, *SHELXTL*, version 5.1, University of Göttingen, Germany, **1999**.

Received December 19, 2002

